Rapid Communications

Energy-level alignment of a single molecule on ultrathin insulating film

Miyabi Imai-Imada,[1,2] Hiroshi Imada,[1] Kuniyuki Miwa,[1,*] Jaehoon Jung,[1,†] Tomoko K. Shimizu,[1,‡] Maki Kawai,[2,§] and Yousoo Kim[1,‖]

[1]*Surface and Interface Science Laboratory, RIKEN, 2-1 Hirosawa, Wako, Saitama 351-0198, Japan*

[2]*Department of Advanced Materials Science, School of Frontier Sciences, The University of Tokyo, 5-1-5 Kashiwanoha, Kashiwa, Chiba 277-8561, Japan*

(Received 10 August 2018; revised manuscript received 14 October 2018; published 15 November 2018)

Elucidation of the energy-level alignment mechanism at a molecule/insulator/metal interface is a key to understanding the molecular and interfacial phenomena. Herein, we provide a detailed investigation into the electronic structures of a free-base phthalocyanine on NaCl films of various thicknesses using scanning tunneling microscopy/spectroscopy (STM/STS). The energy of the ionization and the affinity levels of the molecule were deduced from the STS spectra, and we determined their dependence on the NaCl-film thickness, which can be explained based on three effects: a voltage drop within the NaCl films, the degree of electric-field screening around the molecule, and a variation in the work function of the substrates. We further found that the energy levels relative to the vacuum level are independent of the work function of the substrate, and that the size of the energy gap increases with the thickness. Our results suggest that it is possible to predict the energy levels at the interfaces based on the energy levels of the molecules in a gas phase, the work function of the substrate, and the thickness of the insulating films.

DOI: 10.1103/PhysRevB.98.201403

The alignment of the ionization and the affinity levels of a molecule with respect to the adsorbent, i.e., the energy-level alignment (ELA), at a molecular interface plays a crucial role in understanding the molecular and interfacial phenomena, such as the catalytic reactions, molecular luminescence, charge transport, and charge exchange through the interface [1,2]. The ELA has been extensively investigated mainly at the molecule/metal and molecule/bulk-insulator interfaces. At the molecule/metal interfaces, interfacial interactions, such as a charge transfer between the molecule and the metal, shift the charge neutrality level of the molecule toward the Fermi level (E_F) of the metal substrate [3,4]. In contrast, at the molecule/bulk-insulator interface where the ionization and affinity levels of the molecules are located in the band gap of the insulator, no charge transfer can occur. In such a case, the energy levels of the molecule are not drastically changed upon the adsorption, and thus the energy differences between the molecular energy levels and the vacuum level (E_v) are preserved.

A different type of molecular interface, namely, a molecule/insulator/metal interface, is prepared by forming insulating films of a few atoms in thickness on metal substrates, upon which the molecules are only weakly coupled or decoupled with the underlying metal substrates. The molecules at this interface show novel phenomena that have not been previously observed on metal surfaces, such as reaction pathway control [5,6], molecular luminescence [7–11], and a manipulation of the charge states of the adsorbates [12–15]. Molecule/insulator/metal interfaces are classified between two extreme systems in terms of the degree of interaction between the molecule and metal, which can be varied according to the thickness of the insulating film between them. Thus, to describe the ELA at a molecule/insulator/metal interface, it is necessary to know the energies of the molecular levels with respect to both E_F and E_v of the substrates as a function of the film thickness, which has yet to be quantitatively clarified.

Scanning tunneling microscopy/spectroscopy (STM/STS) have been used for an investigation of the ELA of isolated molecules on ultrathin insulating films [15–18]. However, it has been reported that the peak positions observed in the differential conductance (dI/dV) spectra of molecules adsorbed on insulating films are significantly affected by the tip-sample distance [19,20]. The peak shift in the dI/dV spectra was ascribed to the voltage drop taking place in the insulating layer [19]. Therefore, to correctly describe the ELA at the molecule/insulator/metal interface, it is crucial to compensate the peak shift induced by the voltage drop. In addition, a direct measurement of the work function is necessary to determine the energies of the molecular levels with respect to E_v.

In this Rapid Communication, we propose a general description of the ELA for an isolated single organic molecule adsorbed on a thin insulating film grown on a metal substrate,

*Present address: Department of Chemistry and Biochemistry, University of California San Diego, 9500 Gilman Dr., La Jolla, CA 92093.

†Present address: Department of Chemistry, University of Ulsan, 93 Daehak-ro, Nam-gu, Ulsan 680-749, Republic of Korea.

‡Present address: Department of Applied Physics and Physico-Informatics Faculty of Science and Technology, Keio University, 3-14-1 Hiyoshi, Kouhoku-ku, Yokohama, Kanagawa, 223-8522, Japan.

§Present address: Institute for Molecular Science, National Institutes of Natural Sciences, 38 Nishigo-Naka, Myodaiji, Okazaki 444-8585, Japan.

‖Corresponding author: ykim@riken.jp

which is rationalized through a systematic analysis of the *dI*/*dV* spectra measured on free-base phthalocyanine (H_2Pc) adsorbed on NaCl films of various thicknesses. The peak shift in the *dI*/*dV* spectra arising from the voltage-drop effect is compensated by modeling the tunneling junction as a parallel plane capacitor partially filled with a dielectric material [19,20]. Furthermore, the energy of the ionization level (E_i^v) and the affinity levels (E_a^v) from E_v were determined based on the work functions derived from the measurement of the *dZ*/*dV* spectroscopy. These analyses demonstrate that, while the energy gap ($E_i^v - E_a^v$) monotonously increases with an increase in the thickness of NaCl, the energetic position of the gap center $\frac{E_i^v + E_a^v}{2}$ is aligned despite the work functions of the substrates having a dependence on the thickness of the NaCl film. Our findings suggest that the energy levels of molecule decoupled from a metal substrate can be predicted using the energy levels of the molecule in the gas phase, the thickness of the insulating film, and the work function of the substrate.

All measurements were conducted using a low-temperature STM (Omicron) operated at 4.7 K under an ultrahigh vacuum ($\sim 7 \times 10^{-11}$ Torr) using electrochemically etched W tips. Single-crystal surfaces of Au(111) and Ag(111) were cleaned through repeated cycles of Ar^+ ion sputtering and annealing [10,11]. Deposition of NaCl films onto the crystal surfaces was conducted using a homemade evaporator heated at 900 K [10], while the substrate was held at room temperature. The sample was cooled down to 4.7 K in the STM head, followed by exposure of the evaporated H_2Pc using another evaporator heated at 675 K. The temperature of the sample surface during the evaporation was kept at below 10 K. The *dI*/*dV* spectra, which represent electronic structures near E_F of the substrates, were measured using a standard lock-in technique with a bias voltage modulation of 10 mV [Fig. 2(a)] or 0 mV [Fig. 3(a)] at 617 Hz while opening the feedback loop. The distance between the STM tip and the metal surface (Z) was measured as a function of the bias voltage applied to the sample (V_s), with the feedback closed to obtain the *dZ*/*dV* spectra, which is related to the work function of the substrate, as based on a numerical differentiation of the Z-V_s curves. The spatial distribution of the *dI*/*dV* signals (*dI*/*dV* map) was recorded in a constant height mode with the feedback loop open.

Figure 1(a) shows a large-scale STM image of as-grown NaCl islands on Au(111), where islands of 1 and 2 monolayers (MLs) (100)-terminated NaCl films can be observed. The apparent height of the 1 and 2 ML films are 200 and 350 pm under the scanning conditions, respectively. After annealing the sample to 370 K, the NaCl islands grow thicker, the apparent height of which is 650 nm, corresponding to NaCl(4 ML) [Fig. 1(b)] [21]. Because a Au(111) herringbone reconstruction is observed in all STM images through the NaCl films, the reconstruction beneath the NaCl islands is preserved, indicating a relatively small interaction between the NaCl islands and the underlying metal substrate. H_2Pc molecules are deposited on these 1, 2, and 4 ML NaCl films and the bare Au(111) surface. As shown in Fig. 1(c), individual H_2Pc molecules adsorb on the NaCl islands with the molecular plane parallel to the surface, and the orientation of the molecule aligned toward the [001] direction.

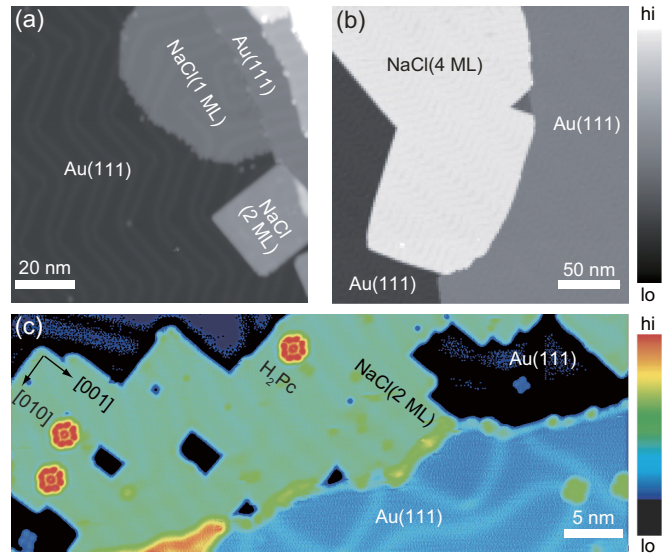

FIG. 1. (a), (b) STM images of NaCl films on Au(111) surface (a) before and (b) after annealing (sample voltage, $V_s = -2.0$ V; tunneling current, $I_t = 4$ pA), and (c) an STM image of H_2Pc/NaCl(2 ML)/Au(111) ($V_s = +1.3$ V, $I_t = 4$ pA).

In the *dI*/*dV* spectra measured on H_2Pc/NaCl(1,2,4 ML)/Au(111) and H_2Pc/Au(111) [Fig. 2(a)], two pronounced peaks corresponding to the affinity and ionization levels can be observed. The molecular orbitals contributing to these levels are visualized using *dI*/*dV* maps acquired at the voltages corresponding to their peaks [Figs. 2(b) and 2(c)]. We noticed that the *dI*/*dV* map of H_2Pc/NaCl/Au(111) measured at the ionization level ($V_s < 0$) is similar to the spatial distribution of the highest occupied molecular orbital (HOMO) in the gas phase calculated through density functional theory (DFT) [Fig. 2(d)], indicating that resonance tunneling through

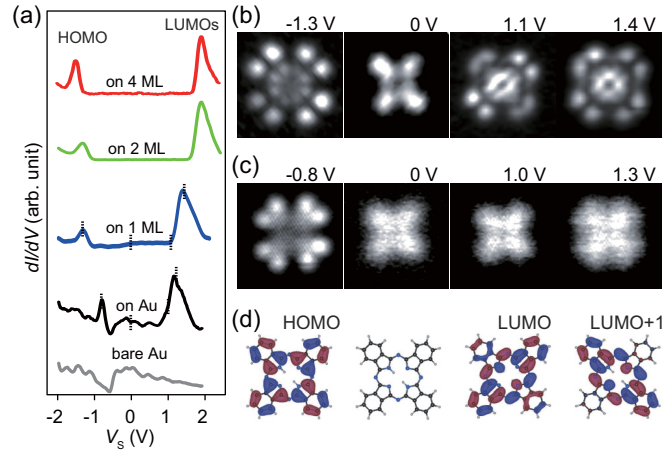

FIG. 2. (a) *dI*/*dV* spectra measured on bare Au(111), H_2Pc/Au(111), and H_2Pc/NaCl(1,2,4 ML)/Au(111). (b), (c) *dI*/*dV* maps of (b) H_2Pc/NaCl(1 ML)/Au(111) and (c) H_2Pc/Au(111) imaged at V_s pointed at in (a). The measurement was conducted in constant height mode. The image sizes are 3.5×3.5 nm^2. (d) Molecular structure of H_2Pc and DFT calculation results of the spatial distributions of the HOMO, LUMO, and LUMO+1 of H_2Pc in the gas phase.

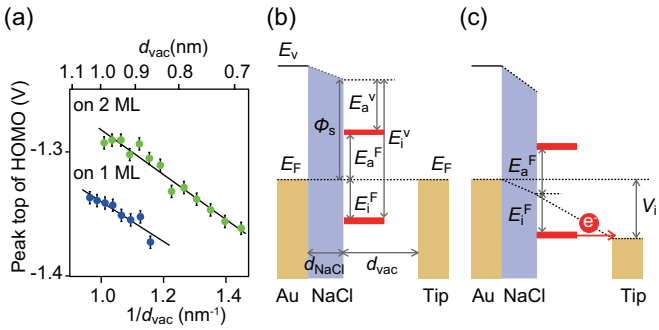

FIG. 3. (a) Plot of the peak top position of the HOMO (V_i) in the *dI/dV* spectrum as a function of $1/d_{vac}$, where d_{vac} is the distance between the tip and the NaCl films as defined in (b). (b), (c) Schematic illustration of the energy diagrams at $V_s = 0$, and at $V_s = V_i$, respectively. The error bars indicate a two-sided 95% confidence interval.

the HOMO is responsible for the *dI/dV* peak of the ionization level. Interestingly, at the affinity level ($V_s > 0$) of H_2Pc/NaCl/Au(111), a slight difference in bias voltage results in different appearances in the *dI/dV* maps. At a lower voltage near the threshold of the affinity levels, the *dI/dV* distribution has twofold symmetry, which is similar to the lowest unoccupied molecular orbital (LUMO). As the voltage is increased to the peak top, the *dI/dV* map reaches quasi-fourfold symmetry. The former twofold symmetry can be explained through a lift of degeneracy of LUMO and LUMO+1. Note that the degeneracy of LUMO and LUMO+1 is lifted in H_2Pc because the molecular symmetry is decreased by the two hydrogen atoms at the molecular center, which is in contrast to the case of metal- Pcs with fourfold symmetry, such as MgPc and CuPc, where LUMO has fourfold symmetry. The latter quasi-fourfold symmetry cannot be explained only through LUMO or LUMO+1; however, we believe that it visualizes both LUMO and LUMO+1 because of the small energy difference between them (∼0.2 eV) [22] and the broad resonance in the *dI/dV* measurement.

In the *dI/dV* maps of H_2Pc/Au(111) [Fig. 2(c)], the distribution observed in the ionization level ($V_s < 0$) has a fourfold symmetry, which is consistent with HOMO in the gas phase. However, the nodal structure is more fuzzy on Au(111) than those of H_2Pc/NaCl/Au(111). The *dI/dV* maps at the affinity level ($V_s > 0$) and within the gap ($V_s = \sim 0$) show a cross shape with a small V_s dependency, which is quite different from the intrinsic MOs. These observations indicate that, although the intrinsic characteristics of the MOs are partially preserved on the inert Au(111), there is a considerable hybridization between the MOs and the electronic states of the Au(111) surface.

These peak positions in the *dI/dV* spectra are not fixed, and shift depending on the measurement conditions, specifically the tip-NaCl surface distance (d_{vac}) [Fig. 3(a)]. By approaching the STM tip toward the substrate, the ionization peaks measured on the H_2Pc/NaCl/Au(111) shift toward the lower voltage side, and the gaps between the ionization and affinity levels increase. Such a shift in peak was not observed on the H_2Pc/Au(111). These results suggest that the peak positions in the *dI/dV* spectra measured at the molecule/insulator/metal interfaces are determined not only by the intrinsic energy levels of the molecules but also by another factor dependent on d_{vac}. Therefore, we decided to conduct a detailed analysis of the *dI/dV* spectra to know the intrinsic energy levels.

It is reasonable to assume that the shift in the *dI/dV* spectrum is caused by a voltage drop within the NaCl films [19,20], which is schematically illustrated in Figs. 3(b) and 3(c). Because the voltage drop is induced by a finite V_s [Fig. 3(c)], the intrinsic energy levels at $V_s = 0$ V [Fig. 3(b)] should be deduced by compensating the voltage drop. By modeling the tunneling junction as a parallel plane capacitor partially filled with NaCl, the peak positions observed in the *dI/dV* spectra (V_η) are correlated with their energy levels at $V_s = 0$ V (E_η) through the following equation [19].

$$V_\eta = \frac{d_{\mathrm{NaCl}} E_\eta}{\varepsilon_r} \frac{1}{d_{\mathrm{vac}}} + E_\eta \quad (\eta = a \text{ or } i). \tag{1}$$

Here, V_a (V_i) is the observed peak position of the affinity (ionization) level, and E_a (E_i) is the energy of the affinity (ionization) level at $V_s = 0$ V with respect to E_F of the substrate. In addition, ε_r is the relative dielectric constant of NaCl films, and d_{NaCl} is the thickness of the films. This model fits our results well, which show a linear relation of V_i as a function of $1/d_{vac}$ [Fig. 3(a)]. The fitted parameters are given by $V_i = -\frac{0.16}{d_{vac}} - 1.18$ on NaCl(1 ML) and $V_i = -\frac{0.18}{d_{vac}} - 1.10$ on NaCl(2 ML). Equation (1) shows that the slope corresponds to $\frac{dE_\eta}{\varepsilon_r}$, and that the intercept corresponds to E_η.

The values of E_i are directly obtained from the intercept in the plots. From the slope of the plots, we estimated ε_r as 2.1 and 3.5 for NaCl(1 ML) and NaCl(2 ML), respectively, using d_{NaCl} values of 288 pm (1 ML) and 576 pm (2 ML) from the crystal structure. The estimated ε_r values of NaCl films on Au(111) are smaller than the value of bulk NaCl, i.e., 5.9 [23], and become smaller as the NaCl-film thickness decreases. The thickness dependency of ε_r is due to the size effect in a thin film structure [24], and the estimated values are comparable with the previously reported ε_r values of 2.0 and 3.2 for 1 and 2 ML NaCl on Ag(100), respectively [25]. The values of E_a are deduced from the *dI/dV* peak position using the estimated ε_r values. For estimating E_a and E_i on NaCl(4 ML), we used the ε_r value of the bulk NaCl instead of an experimentally determined value. A direct measurement of ε_r of NaCl(4 ML)/Au(111) is difficult because the molecules on relatively thick and slightly conductive films were easily attached to the STM tip when d_{vac} was reduced, which prevented us from obtaining the *dI/dV* peak shift within a sufficiently wide range of d_{vac} to determine ε_r. The use of the bulk value is rationalized by a theoretical study [24] which has shown that ε_r values saturate to the bulk values quickly when the thicknesses become thicker, especially if the bulk values are smaller than 10 as is the case for NaCl. The estimated values of E_a and E_i are summarized in Table I.

We denote the intrinsic energy levels of the molecule with respect to E_F of the substrate as E_η^F ($\eta = a$ or i), and plot the values in Fig. 4(a). Because the plot does not reveal a systematic dependence on the film thickness, we instead determined the ionization and affinity levels with respect to E_v through a measurement of the work function of the substrates [Φ_s in Fig. 3(b)]. The value of $\Phi_{Au(111)}$ is

TABLE I. E_a^F, E_i^F, ε_r, and parameters used in the calculations.

Substrate	ε_r	d_{vac}[a] (pm)	d_{NaCl}[b] (pm)	V_a (eV)	V_i (eV)	E_a^F (eV)	E_i^F (eV)	$E_a^F - E_i^F$ (eV)
Au(111)		750		1.20	−0.80	1.20	−0.80	2.00
NaCl(1 ML)	2.1	774	288	1.39	−1.33	1.18	−1.18	2.36
NaCl(2 ML)	3.5	777	576	1.76	−1.40	1.45	−1.10	2.56

[a]The tip-surface distance or the thickness of the vacuum gap in the tunneling junction [Fig. 3(b)]. The tip height refers to the point contact between the tip and the metal surface.
[b]Distance between neighboring [100] planes in a NaCl single crystal.

modified through thin film growth owing to the formation of an interfacial dipole under the thin film. Such work function changes from a bare metal surface have been determined through an observation of Gundlach oscillation [26,27] in differential *Z*/*V* spectra using STM [Fig. 4(b)]. A Gundlach oscillation is a series of standing-wave states formed in a tunneling gap, and the difference in work function between two surface regions is derivable from the shift in the Gundlach

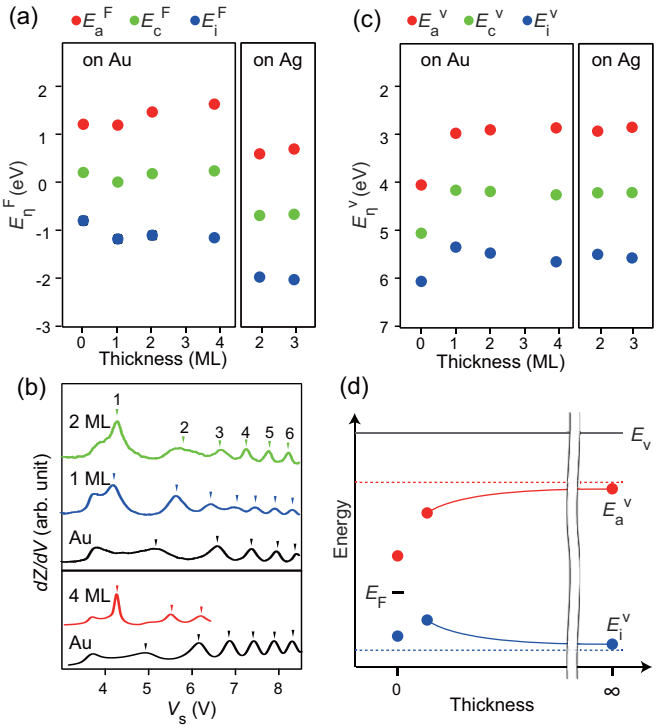

FIG. 4. (a) Energies of the ionization and affinity levels with respect to E_F. (b) *dZ*/*dV* spectra of 1 ML (blue), 2 ML (green), and 4 ML (red) NaCl films and bare Au(111) (black) as a reference. The orders of the field emission resonances are assigned from the lowest voltage. (c) Energies of the ionization and affinity levels with respect to E_v. (d) A schematic illustration of the ELA of a molecule on an insulating film supported by a metal substrate as a function of the thickness of the insulating film. The two extremes, thickness = 0 and infinity, correspond to the cases with a molecule adsorbed directly on metal substrate or on the bulk insulator, respectively. The dashed lines represent the ionization potential (blue), and the electron affinity (red) of the molecule in the gas phase. The Fermi levels of the bare metal substrate are shown by a black line.

oscillation patterns [25,27–29]. In the *dZ*/*dV* spectra shown in Fig. 4(b), the peaks marked by the triangles correspond to the standing-wave states, which are considerably shifted toward the lowered voltage side on the NaCl from those on Au(111). The differences in the work function between the Au(111) and NaCl/Au(111) were deduced from the averaged shifts of the standing-wave states as 1.09, 0.89, and 0.77 eV for 1, 2, and 4 ML, respectively. The energetic position of the affinity and ionization levels at $V_s = 0$ V with respect to E_v are denoted as E_η^v ($\eta = a$ or i) and are correlated with E_η^F through $E_\eta^v \equiv \phi_s - E_\eta^F$. The values of E_η^v and the center of these levels $E_c^v \equiv \frac{E_i^v + E_a^v}{2}$ are plotted in Fig. 4(c), which reveals clear tendencies. First, the energy gap $(E_i^v - E_a^v)$ increases with the thickness of the NaCl film. Second, the energy of E_c^v is constant regardless of the work function of the substrates, except for H_2Pc/Au(111). The change in gap size can be explained by the screening of the electric field around the tentatively ionized molecule from the underlying metal substrates, which reduces the Coulomb potential. The screening effect is expected to decrease with the increase in the molecule-metal distance as determined by the film thickness [30], which is consistent with our observations and a previously reported theoretical investigation [31]. The invariance of E_c^v indicates the "vacuum-level alignment" of both the ionization and affinity levels [32], which has been observed when the electronic states of adsorbates are decoupled from the metal substrates. In contrast, E_c^v of H_2Pc/Au(111) are shifted toward E_F of the substrate, 5.31 eV, suggesting a considerable hybridization between the MOs and the electronic states of the Au(111) surface. These results demonstrate that only a few atomic layers of insulating materials are sufficient to decouple a molecule, and that the energy levels still receive a long-range screening effect from the metal.

Figure 4(d) shows a schematic illustration of the ELA of the molecule/insulator/metal interface as well as molecule/metal and molecule/bulk-insulator interfaces. At a molecule/metal interface (thickness = 0), E_η^v shifts toward E_F of the metal substrate as a result of interfacial interaction, such as charge transfer and orbital hybridization between a molecule and a metal [2,33]. In contrast, at a molecule/bulk-insulator interface (thickness $\to \infty$), no charge transfer occurs when E_a^v and E_i^v are in the band gap of the insulator. Although the molecular energy levels are not drastically changed upon the adsorption, the insulator is expected to reduce the energy gap between E_a^v and E_i^v as a result of reorganization [34,35]. As discussed above, the ELA at the molecule/insulating film/metal interface is described by a vacuum-level alignment combined with the screening effect. This description for the finite film thickness is different from that for the well-studied two extreme cases. When increasing the thickness, the ionization (affinity) level originating from a tentative charged state shifts downward (upward) owing to the reduced screening from the metal. The center of these levels with respect to E_v remains unchanged from the bulk insulator to the ultrathin limit.

Our model suggests predictability of the value of E_c^v on thin insulating films based on the energy levels of the molecule in the gas phase. Actually, E_i^v and the energy gap $(E_i^v - E_a^v)$ of H_2Pc in the gas phase are 6.4 [36] and

4.12 eV [37], respectively. The resulting E_c^v calculated from these values is 4.34 eV, which is in good agreement with our result, namely, 4.26 ± 0.09 eV. Moreover, the energy gap at a molecule/insulator/metal interface can be estimated by a theoretical method based on a simple dielectric model [34]. Another support of our model is based on an additional experiment conducted with H_2Pc/NaCl(2,3 ML)/Ag(111), which have work functions of 3.58 and 3.57 eV, respectively (see Supplemental Material [38]). The experiment results are shown in Supplmental Material Fig. S1 and Figs. 4(a) and 4(c). Measuring *dI*/*dV* spectra followed by the compensation of the voltage drop using d_{NaCl}, and ε_{r} (3.2 for 2 ML, 3.5 for 3 ML [25]), the values of E_i^F and E_a^F are found to be −1.93 and 0.58 eV on 2 ML, and −2.02 and 0.69 eV on 3 ML, respectively [the right panel of Fig. 4(a)]. The values of E_i^v and E_a^v are calculated using E_η^F and the work functions as 5.51 and 3.00 eV for 2 ML, and 5.59 and 2.88 eV for 3 ML, respectively, as shown in the right panel of Fig. 4(c). Despite considerable work function difference from NaCl/Au(111), the values of E_c^v on NaCl(2,3 ML)/Ag(111) are identical within the margin of error. Moreover, the gap size on NaCl(3 ML)/Ag(111) is larger than that on NaCl(2 ML)/Ag(111), which is expected according to our model.

In conclusion, we have clarified the mechanism of the ELA of an isolated H_2Pc on NaCl films grown on metal substrates using STM/STS. Despite the variation in work function among the substrates with NaCl films of different thicknesses on Au(111) and Ag(111), the value of E_c^v on the insulating films was found to be constant. In addition, the energy gap between the energy levels increases as thickness of the NaCl film increases. These observations are explained through the vacuum-level alignment and electric-field screening from the metal substrate. Our findings allow us to control the charge injection barriers using the energy levels of the molecule in the gas phase, the work function of the substrate, and the thickness of the film. It is also suggested that the charge injection barriers can be tuned by applying an external electric field from the STM tip [19,39]. These insights will be very useful for selecting the combination of organic material and substrate in an organic electronic device to optimize the charge injection efficiency.

We thank Emi Minamitani, Chun-Liang Lin, Ryuichi Arafune, and Holly Walen for their helpful discussions. This work was supported in part by JSPS KAKENHI (Grants No. 21225001, No. 15H02025, No. 17H04796, No. 17H05470, No. 17K18766, No. 26886013, No. 16K21623, No. 18H05257, and No. 15J03915). M. I. I. was supported by JSPS through Program for Leading Graduate Schools (MERIT), and the RIKEN Junior Research Associate Program.

[1] T. Yokoyama, D. Yoshimura, E. Ito, H. Ishii, Y. Ouchi, and K. Seki, Jpn. J. Appl. Phys. **42**, 3666 (2003).
[2] S. Braun, W. R. Salaneck, and M. Fahlman, Adv. Mater. **21**, 1450 (2009).
[3] H. Vázquez, F. Flores, R. Oszwaldowski, J. Ortega, R. Pérez, and A. Kahn, Appl. Surf. Sci. **234**, 107 (2004).
[4] H. Vázquez, R. Oszwaldowski, P. Pou, J. Ortega, R. Pérez, F. Flores, and A. Kahn, Europhys. Lett. **65**, 802 (2004).
[5] H.-J. Shin, J. Jung, K. Motobayashi, S. Yanagisawa, Y. Morikawa, Y. Kim, and M. Kawai, Nat. Mater. **9**, 442 (2010).
[6] J. Repp, G. Meyer, S. Paavilainen, F. E. Olsson, and M. Persson, Science **312**, 1196 (2006).
[7] X. H. Qiu, G. V Nazin, and W. Ho, Science **299**, 542 (2003).
[8] F. Rossel, M. Pivetta, and W.-D. Schneider, Surf. Sci. Rep. **65**, 129 (2010).
[9] K. Kuhnke, C. Große, P. Merino, and K. Kern, Chem. Rev. **117**, 5174 (2017).
[10] H. Imada, K. Miwa, M. Imai-Imada, S. Kawahara, K. Kimura, and Y. Kim, Nature (London) **538**, 364 (2016).
[11] H. Imada, K. Miwa, M. Imai-Imada, S. Kawahara, K. Kimura, and Y. Kim, Phys. Rev. Lett. **119**, 013901 (2017).
[12] W. Steurer, J. Repp, L. Gross, I. Scivetti, M. Persson, and G. Meyer, Phys. Rev. Lett. **114**, 036801 (2015).
[13] F. E. Olsson, S. Paavilainen, M. Persson, J. Repp, and G. Meyer, Phys. Rev. Lett. **98**, 176803 (2007).
[14] J. Repp, G. Meyer, F. E. Olsson, and M. Persson, Science **305**, 493 (2004).
[15] I. Swart, T. Sonnleitner, and J. Repp, Nano Lett. **11**, 1580 (2011).
[16] J. Repp, G. Meyer, S. M. Stojković, A. Gourdon, and C. Joachim, Phys. Rev. Lett. **94**, 026803 (2005).
[17] P. Liljeroth, J. Repp, and G. Meyer, Science **317**, 1203 (2007).
[18] S. Koslowski, D. Rosenblatt, A. Kabakchiev, K. Kuhnke, K. Kern, and U. Schlickum, Beilstein J. Nanotechnol. **8**, 1388 (2017).
[19] S. W. Wu, G. V. Nazin, X. Chen, X. H. Qiu, and W. Ho, Phys. Rev. Lett. **93**, 236802 (2004).
[20] N. Nilius, Surf. Sci. Rep. **64**, 595 (2009).
[21] C. Bombis, N. Kalashnyk, W. Xu, E. Laegsgaard, F. Besenbacher, and T. R. Linderoth, Small **5**, 2177 (2009).
[22] K. Toyota, J. Hasegawa, and H. Nakatsuji, J. Phys. Chem. A **101**, 446 (1997).
[23] M. C. Robinson and A. C. H. Hallett, Can. J. Phys. **44**, 2211 (1966).
[24] K. Natori, D. Otani, and N. Sano, Appl. Phys. Lett. **73**, 632 (1998).
[25] H.-C. Ploigt, C. Brun, M. Pivetta, F. Patthey, and W.-D. Schneider, Phys. Rev. B **76**, 195404 (2007).
[26] K. H. Gundlach, Solid State Electron. **9**, 949 (1966).
[27] C. L. Lin, S. M. Lu, W. B. Su, H. T. Shih, B. F. Wu, Y. D. Yao, C. S. Chang, and T. T. Tsong, Phys. Rev. Lett. **99**, 216103 (2007).
[28] M. Pivetta, F. Patthey, M. Stengel, A. Baldereschi, and W.-D. Schneider, Phys. Rev. B **72**, 115404 (2005).
[29] W. B. Su, S. M. Lu, C. L. Lin, H. T. Shih, C. L. Jiang, C. S. Chang, and T. T. Tsong, Phys. Rev. B **75**, 195406 (2007).
[30] M. Strange and K. S. Thygesen, Phys. Rev. B **86**, 195121 (2012).
[31] C. Freysoldt, P. Rinke, and M. Scheffler, Phys. Rev. Lett. **103**, 056803 (2009).
[32] G. Witte, S. Lukas, P. S. Bagus, and C. Wöll, Appl. Phys. Lett. **87**, 263502 (2005).

[33] H. Ishii, K. Sugiyama, E. Ito, and K. Seki, Adv. Mater. **11**, 605 (1999).
[34] I. Scivetti and M. Persson, J. Phys.: Condens. Matter **29**, 355002 (2017).
[35] S. Fatayer, B. Schuler, W. Steurer, I. Scivetti, J. Repp, L. Gross, M. Persson, and G. Meyer, Nat. Nanotechnol. **13**, 376 (2018).
[36] J. Berkowitz, J. Chem. Phys. **70**, 2819 (1979).
[37] X. Blase, C. Attaccalite, and V. Olevano, Phys. Rev. B **83**, 115103 (2011).
[38] See Supplemental Material at http://link.aps.org/supplemental/10.1103/PhysRevB.98.201403 for a description on additional experimental data and discussions about the molecular energy levels on the NaCl(2,3 ML)/Ag(111).
[39] G. V Nazin, S. W. Wu, and W. Ho, Proc. Natl. Acad. Sci. USA **102**, 8832 (2005).